The homodimeric GBS1074 from *Streptococcus agalactiae*

Anshuman Shukla,[a]‡ **Mark Pallen,**[a] **Mark Anthony**[a,b]§ **and Scott A. White**[a]*

[a]School of Biosciences, University of Birmingham, Edgbaston, Birmingham B15 2TT, England, and [b]Birmingham Women's NHS Foundation Trust, Edgbaston, Birmingham B15 2TG, England

‡ Current address: School of Medicine, University of Birmingham, Edgbaston, Birmingham B15 2TT, England.
§ Current address and correspondence for microbiology: The Neonatal Unit, John Radcliffe Hospital, Oxford OX3 9DU, England. E-mail: mark.anthony@orh.nhs.uk.

Correspondence e-mail: s.a.white@bham.ac.uk

ESAT-6 is a well characterized secreted protein from *Mycobacterium tuberculosis* and represents the archetype of the WXG100 family of proteins. Genes encoding ESAT-6 homologues have been identified in the genome of the human pathogen *Streptococcus agalactiae*; one of these genes, *esxA*, has been cloned and the recombinant protein has been crystallized. In contrast to *M. tuberculosis* ESAT-6, the crystal structure of GBS1074 reveals a homodimeric structure similar to homologous structures from *Staphylococcus aureus* and *Helicobacter pylori*. Intriguingly, GBS1074 forms elongated fibre-like assemblies in the crystal structure.

1. Introduction

The secreted proteins ESAT-6 (early secreted antigen target 6) and CFP10 (culture filtrate protein 10) from *Mycobacterium tuberculosis* play a key role in virulence and elicit a strong antigenic response (forming the basis of a new diagnostic test), although their precise biological function has yet to be defined. NMR (Renshaw *et al.*, 2005; PDB code 1wa8) and crystal (Poulsen *et al.*, 2010; PDB code 3fav) structures have confirmed that the two proteins are homologous to one another and form a tight 1:1 heterodimeric complex composed of antiparallel helical hairpins arranged in a head-to-tail fashion and held together by a predominantly hydrophobic interface. Pallen (2002) used sequence analyses to show that ESAT-6 and CFP10 are archetypes of a large family of WXG100 proteins (so-called because of their central W*X*G amino-acid motif and a length commonly of ∼100 amino acids), members of which are widely distributed among Gram-positive bacteria. Drawing on these observations, Burts *et al.* (2005) showed that WXG100 proteins contribute to virulence in *Staphylococcus aureus*. Subsequently, crystal structures of WXG100 proteins from *S. aureus* (Sundaramoorthy *et al.*, 2008; PDB codes 2vs0 and 2vrz) and *Helicobacter pylori* (Jang *et al.*, 2009; PDB codes 3fx7 and 2gts) have shown these proteins to form homodimeric head-to-tail structures. Most recently, the *M. tuberculosis* Rv3019c–Rv3020c ESX complex has been shown to form both heterodimers and heterotetramers in solution in a relative ratio of approximately 15:1, but only the heterotetrameric complex could be crystallized (Arbing *et al.*, 2010; PDB code 3h6p). The EsxR protein (the ESAT-6 homologue) folds as an antiparallel helical hairpin as expected, but strikingly the EsxS protein (the CFP10 homologue) folds as one long extended helix, with the C-terminal half of the helix domain-swapping with that of a second equivalent EsxRS complex to form a heterotetramer composed of two four-helix bundles (see Fig. 2 of Arbing *et al.*, 2010).

Streptococcus agalactiae (group B streptococcus; GBS) is a leading cause of neonatal sepsis and infections in pregnant women (Larsen & Sever, 2008) and can also cause invasive infection in other settings (Sendi *et al.*, 2008). Given the contribution of WXG100 proteins to virulence in *M. tuberculosis* and *S. aureus*, we searched for additional members of this protein family in the predicted proteome of *S. agalactiae* strain NEM316 (Herbert *et al.*, 2005). We solved the crystal structure of one such protein, GBS1074, to 2.0 Å resolution. As with related WXG100 proteins from *S. aureus* and *H. pylori*, GBS1074 adopts a homodimeric structure, but intriguingly the crystal packing suggests the potential to form higher order polymers, with a

second intermolecular interface being formed between the extended C-terminal helical regions.

2. Experimental

2.1. General methods

S. agalactiae strains were cultured in Todd–Hewitt broth and on Todd–Hewitt agar and *Escherichia coli* was cultured in LB medium. Genome, gene and protein analyses were performed with *x*BASE2 (http://xbase.bham.ac.uk/; Chaudhuri *et al.*, 2008), *PSI-BLAST* and *ClustalW* (http://www.ebi.ac.uk/Tools). Genomic DNA was extracted with a DNeasy Blood and Tissue kit (Qiagen).

2.2. Cloning and expression of GBS1074

The GBS1074 coding sequence was amplified with primers GBS1074f_*Bam*HI (5′-TAC GGA TCC ATG GCA CAA ATT AAA TTA ACA CC-3′) and GBS1074r_*Sal*I (5′-GTC GAC GTA TCC ACT AAT TTG AGA AGC-3′) and cloned into pQE-80 (Qiagen) and recombinant GBS1074 protein with an N-terminal MRGS-HHH-HHH-GS tag was expressed in *E. coli* XL1-Blue (Stratagene) at 293 K. Cells were induced with 1 mM IPTG at an OD_{600} of 0.6 and then cultured overnight at 293 K. Harvested cells were suspended in lysis buffer (50 mM NaH$_2$PO$_4$ pH 8.0, 300 mM NaCl, 10 mM imidazole) and lysed using a French press. The lysate was centrifuged at 18 000g for 1 h and the supernatant was loaded onto an Ni–NTA column, washed (50 mM NaH$_2$PO$_4$ pH 8.0, 300 mM NaCl, 20 mM imidazole) and eluted (50 mM NaH$_2$PO$_4$ pH 8.0, 300 mM NaCl, 250 mM imidazole). The protein was dialysed against 20 mM Tris pH 8.0 to remove imidazole. The histidine tag was not removed.

2.3. Crystallization, data collection and structure determination

Crystals of GBS1074 were prepared using the sitting-drop vapour-diffusion technique with a drop consisting of 2 µl protein stock solution (20 mg ml^{-1} GBS1074, 10 mM Tris buffer pH 8) mixed with 2 µl reservoir solution (0.75 M Li$_2$SO$_4$, 0.6 M ammonium sulfate, 0.1 M sodium citrate pH 5.1). Hexagonal-shaped crystals belonging to space group $P6_522$ grew within a few days to a maximum dimension of approximately 0.5 mm. Crystals were transferred to a stabilization solution based on the mother liquor and were then cryoprotected by increasing the concentration of glycerol (in 5% steps to a final concentration of 25%) before flash-cooling and storage in liquid nitrogen. An iodine derivative was obtained by soaking a crystal as above but with a final solution supplemented with 1.9 mM I$_2$ and 2.7 mM KI prepared by using a 250-fold dilution of the KI/I$_2$ stock solution described in Evans & Bricogne (2002). The crystal was left in the derivative solution for 48 h, by which time the crystal was a strong yellow colour and the solution was completely colourless. Higher concentrations of KI/I$_2$ cracked the crystals.

Both 'Native1' and 'Iodine' data sets were collected on our in-house X-ray facility (Rigaku MicroMax-007 HF with Saturn CCD and Kappa four-circle goniometer) with scans around multiple axes. To maximize the anomalous signal contribution from the iodine derivative, a highly redundant data set (~60 h) was collected. A second native data set, 'Native2', was collected on ESRF beamline ID14-1. All data were indexed and integrated with *XDS* (Kabsch, 2010) and scaled using either *SCALA* (Native1 and Native2; Evans, 1993) or *XSCALE* (Iodine; Kabsch, 2010). Merging statistics were calculated in *SCALA* for all three data sets. Iodine positions were located and phases were determined using a SIRAS protocol (Iodine and Native1) with the program *autoSHARP* (Vonrhein *et al.*, 2007),

Table 1
Data-collection and phasing statistics.

Values in parentheses are for the highest resolution shell.

	Native1	Native2	Iodine
Crystal properties			
Space group	$P6_522$	$P6_522$	$P6_522$
Unit-cell parameters (Å)			
$a = b$	77.2	76.2	77.1
c	152.8	151.3	153.7
Data collection			
Wavelength (Å)	1.542	0.933	1.542
No. of observations	873191 (91459)	211669 (30807)	2259118 (303657)
No. of unique reflections	16476 (2344)	18255 (2591)	5881 (818)
Completeness (%)	99.9 (100)	99.7 (100)	99.6 (99.9)
Multiplicity	53 (39)	11.6 (11.9)	384 (371)
Anomalous completeness (%)			99.9 (100)
Anomalous multiplicity			190 (191)
$\langle I/\sigma(I)\rangle$	58.6 (8.4)	34 (6.7)	174.7 (49.3)
Anomalous signal [$|F_+ - F_-|/\sigma(\Delta F)$]			4.7 (1.5)
R_{merge} (%)	5.3 (61.2)	4.2 (39.6)	8.4 (29.9)
Resolution range (Å)	19.5–2.1 (2.21–2.10)	40.1–2.0 (2.11–2.00)	19.5–3.0 (3.16–3.00)
Wilson B (Å^2)	34.2	32.8	63.3
Refinement			
No. of non-H atoms		1616	
No. of waters		140	
R/R_{free}†		18.9/21.9	
R.m.s.d.			
Bonds (Å)		0.006	
Angles (°)		0.742	
Ramachandran‡		172/4/0/0	
Average B (Å^2)		45	
PDB code		3o9o	

† R_{free} was calculated for a random set of 5% of reflections that were not used in the refinement. ‡ Number of nonglycine, nonproline amino acids in the core/allowed/generously allowed/disallowed regions of the Ramachandran plot.

yielding a clear interpretable electron-density map. Six significant iodine sites were located and refined. All six sites showed single I atoms, with no evidence of I$_2$ or I$_3^-$ binding (Evans & Bricogne, 2002); the shortest I—I distance was 6.05 Å. Three of the sites were buried in the hydrophobic interior of the protein, with two being noncrystallographically equivalent. Two further sites were in hydrophobic surface pockets with the potential to also form hydrogen bonds to solvent or protein and one site was located in a pocket formed at the interface of two protein molecules. *RESOLVE* (Terwilliger, 2002) was used to autotrace and build 145 amino acids (backbone and side chain) in four helical fragments, plus an additional 19 amino acids (backbone only) in a further four fragments, representing approximately 85% of the mature nontagged portion of the GBS1074 homodimer. The programs *Coot* (Emsley & Cowtan, 2004) and *phenix.refine* (Afonine *et al.*, 2005) with MLHL targets were used to complete and refine the structure. The resulting refined Native1 structure was then refined against the 2.0 Å resolution Native2 data set. Data-collection and phasing statistics are presented in Table 1. Structural alignments were calculated using *LSQKAB* (Collaborative Computational Project, Number 4, 1994). Contact surfaces were analysed using the *PISA* server (Krissinel & Henrick, 2007) and *AREAIMOL* (Collaborative Computational Project, Number 4, 1994).

3. Results

3.1. WXG100 proteins encoded in the *S. agalactiae* genome

We identified three genes encoding WXG100 proteins in *S. agalactiae* strain NEM316 (GBS0223, GBS1074 and GBS1979; data not shown). The gene encoding GBS1074 lies within a putative

WXG100 secretion-system locus that encompasses homologues of the *S. aureus essC*, *essB* and *esaB* genes, which are essential for secretion of the WXG100 protein EsxA (Pallen, 2002; Burts *et al.*, 2005). GBS1074 bears a canonical central W*X*G motif and shows

14.9% amino-acid identity to ESAT-6 from *M. tuberculosis* and 22.7% amino-acid identity to EsxA from *S. aureus*.

3.2. GBS1074 crystal structure

The crystal structure of recombinant GBS1074 was solved using the SIRAS technique with an iodine derivative (Evans & Bricogne, 2002; Fig. 1). The unbiased electron-density maps resulting from SIRAS phase calculations were of high quality and were easily interpretable, enabling automatic model building for approximately 85% of the Native1 structure, with the remainder being built manually. Owing to structural ambiguity of a few amino acids at the termini, the Native1 structure was refined against a second native data set, Native2, to produce a final model containing amino-acid residues 4–95 in subunit *A* and 0–95 in subunit *B*, where 0 is the last amino acid of the linker between the N-terminal His$_6$ tag and the starting methionine (Table 1). The remainder of the linker and the His$_6$ tags were not visible in the electron density. A portion of the final refined $2F_o - F_c$ electron-density map is shown in Fig. 2.

3.3. Homodimeric structure

There are two molecules per asymmetric unit, forming a homodimer, with each subunit contributing 1850 Å^2 of solvent-accessible surface area to the interface. Owing to the head-to-tail symmetrical nature of the dimer, inter-subunit contacts are preserved in the twofold symmetry; therefore, amino acids in one polypeptide chain
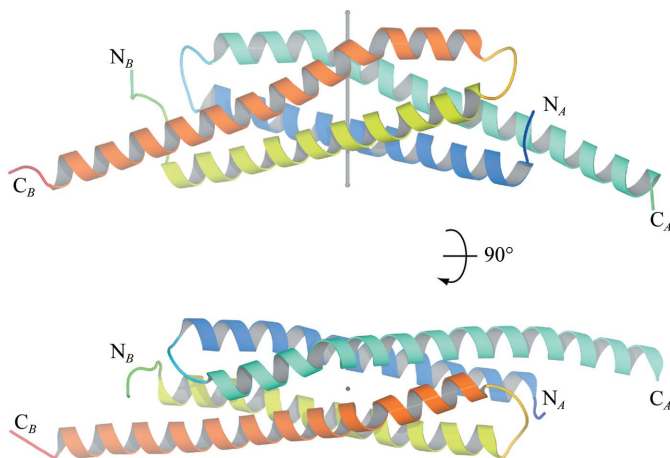

Figure 1
GBS1074 crystal structure. Ribbon diagram of GBS1074 in two orthogonal views. Chain *A* is shown in green and blue and chain *B* in yellow and orange. The twofold NCS axis is indicated in grey.
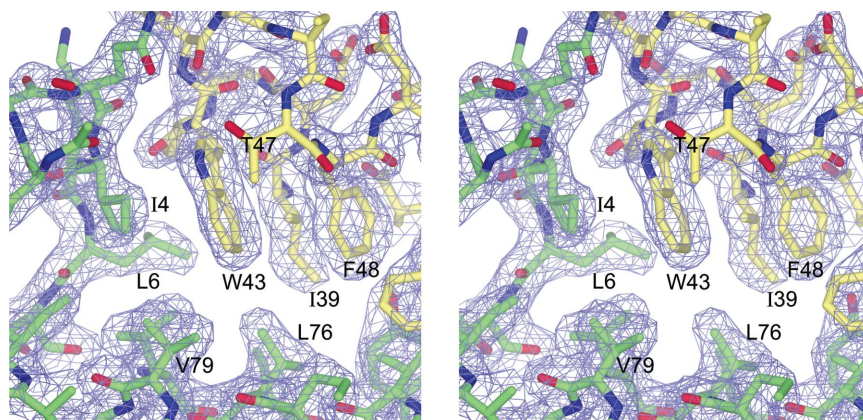

Figure 2
Wall-eyed stereoview of the refined $2F_o - F_c$ electron-density map (contour level 1.2σ) showing part of the hydrophobic core around Trp43. Atoms are coloured as follows: oxygen, red; nitrogen, blue; carbon, yellow (subunit *A*) or green (subunit *B*).
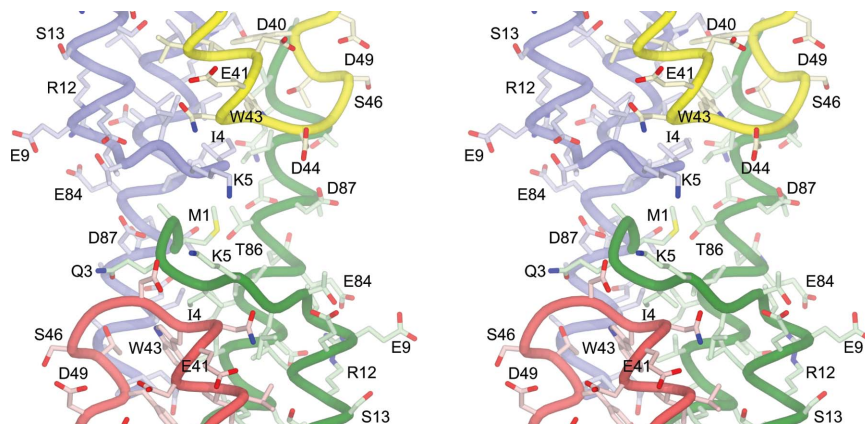

Figure 3
Wall-eyed stereoview of the crystallographic symmetry interactions between one molecule and the next along the chain. Chain *B* is coloured green and chain *A* is coloured red. In the symmetry mate (mostly shown in the upper half of the figure) chain *A* is coloured blue and chain *B* is coloured yellow (see also Fig. 5).

are distinguished from those in the other by a prime ('). The r.m.s.d. between subunits is 1.32 Å when comparing the maximum 92 pairs of C^α atoms, but this improves to 0.62 Å for 85 pairs of C^α atoms when the last seven amino acids of each chain are excluded. Although a continuation of the second helix, the helix axes over the last two helical turns at the C-termini diverge, probably as a result of crystal packing (see below). The homodimer interface is almost exclusively hydrophobic and is further stabilized by peripheral hydrogen bonding and salt bridges in a typical heptad amino-acid repeat.

The GBS1074 protein folds as an antiparallel coiled-coil pair to form a four-helix bundle (Fig. 1) typified by the structure of the protein ROP. Each subunit forms two long helices, Pro8–Glu41 and Asp49–Ile94, with a 30° kink in the second helix at Leu68. Amino acids Trp43-Asp44-Gly45, the conserved WXG motif, form the apex of the loop connecting the antiparallel helices. The side chain of Trp43 is part of an extensive hydrophobic core and Gly45 is the only amino acid in the refined model to be in the lower right-hand corner of the Ramachandran plot, a region that is disallowed for nonglycine amino acids.

The N-terminus of one polypeptide chain interacts with the WXG motif of the other (Figs. 1, 2 and 3). Ile4 forms van der Waals interactions with Trp43′ and together with Leu6 and Met1 (in the B chain only) forms an extension of the hydrophobic core that holds the two pairs of antiparallel helices together into a four-helix bundle. Lys5 and Asp44′, two amino acids that are conserved in many WXG100-family members, form a salt bridge and in the only intersubunit main-chain–main-chain hydrogen bonding in the whole molecule the backbone O atom of Gln3 forms a hydrogen bond to Asp44′ N and Lys5 N hydrogen bonds to Asn42′ O, so that Ile4 forms an inter-subunit β-bridge with Trp43′. Overall, the homodimer is approximately cylindrical, with a diameter of 25 Å and a length of 95 Å, and

has a distinctive negative patch on the surface formed by amino acids Asp40, Asp44, Asp49, Glu52 and, slightly further away, Glu41 (Fig. 4).

4. Discussion

4.1. Structural homology

The available structures of WXG100 proteins are highly similar. While the archetypal pair ESAT-6 and CFP10 form a heterodimer and a minor component of the related *M. tuberculosis* EsxRS complex forms a domain-swapped heterotetramer, other WXG100 proteins of known structure, now including GBS1074, form homodimers. Although the NMR structure of ESAT-6 shows a relatively unstructured C-terminus, with the deviation from regular helicity starting at residue Ala79, this C-terminal region has been described as having a high helical propensity (Renshaw *et al.*, 2005). In the crystal structure of GBS1074, as in the X-ray structure of the ESAT-6–CFP10 complex and in similar structures of WXG100 proteins from *S. aureus* and *H. pylori*, the second helix is continuous until the end of the polypeptide chain. Interestingly, in GBS1074 the C-terminal helical region forms extensive intermolecular contacts with neighbouring molecules (see below).

4.2. Crystal packing and fibre-like structures

A packing analysis of the GBS1074 crystal structure offers the intriguing possibility that GBS1074 can form fibre-like structures (Fig. 5) or some higher order assembly. In the crystal, GBS1074 molecules are aligned end-to-end in a chain fashion, with alternating up–down links. Each homodimer contributes 850 $Å^2$ of solvent-accessible surface area to the interface with the next homodimer along the chain, the second largest interface in the crystal structure (Fig. 5). The protruding C-terminal helices continue the antiparallel coiled-coil interactions along the chain. In addition, the backbone amide of Met1 hydrogen bonds to the conserved Asp87 OD1 (2.6 Å) of a chain-forming symmetry mate, an interaction that would be a salt bridge if the N-terminal tag were not present (Fig. 3). The conserved hydrophobic positions 90 and 94 (both Ile) of one homodimer form van der Waals interactions with Trp43 of another, each contributing approximately 100 $Å^2$ of solvent-accessible surface to the potential fibre-forming interface. Such end-to-end chain interactions were not observed in the crystal structures of EsxA from *S. aureus*, although Sundaramoorthy *et al.* (2008) describe a potential peptide-binding groove on the surface of the protein. Despite positions 90 and 94 in EsxA being hydrophobic (Leu and Phe, respectively), only subunit *A* of PDB entry 2vrz has a structurally ordered C-terminus. The last 10–15 amino acids are disordered in chain *B* of PDB entry 2vrz and in both subunits of PDB entry 2vs0. End-to-end chain interactions are not seen in the crystal structure of HP0062 either, but here the sequence is shorter. The intermolecular interactions observed in the
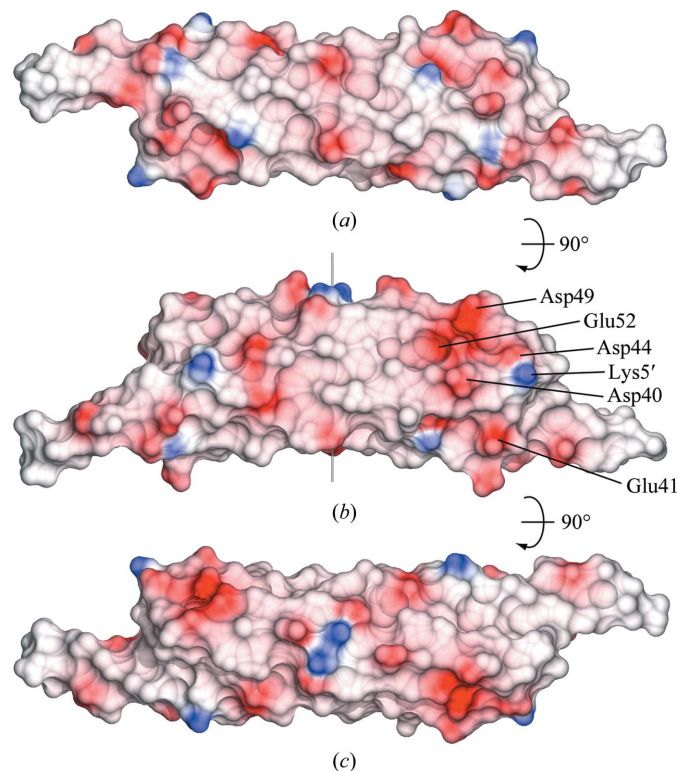
(a)

(b)
— Asp49
— Glu52
— Asp44
— Lys5′
— Asp40
— Glu41

(c)

Figure 4
Molecular surfaces coloured according to electrostatic potential using the program *CCP4MG* with default colour settings (Potterton *et al.*, 2004). (*b*) has the same orientation as Fig. 1(*a*).

NCS   *B*   *A*   NCS
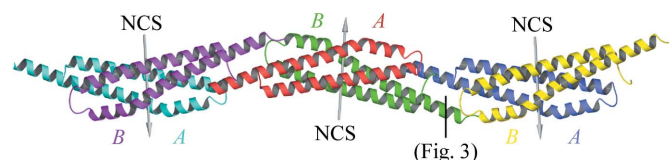*B*   *A*   NCS   *B*   *A*
(Fig. 3)

Figure 5
Crystal packing showing potential chain-forming interactions. NCS, noncrystallographic symmetry. Three dimers in the chain are shown. The asymmetric unit (x, y, z) is the dimer in the centre coloured red and green. The dimer to the left of the figure, coloured cyan and magenta ($x, x - y, -z + 5/6$), and the dimer to the right, coloured blue and yellow ($x, x - y, -z + 5/6$), are related by unit-cell translations ($2a + b$). The *A* and *B* monomers are labelled in matching colours. The interface shown in Fig. 3 is indicated.

GBS1074 crystal structure are reminiscent of the crystal packing and oligomer assembly in the structure of the secreted mature FadA (PDB entry 3etw), a bacterial adhesion protein from the opportunistic human pathogen *Fusobacterium nucleatum* that has been shown to be important for host-cell attachment and invasion (Nithianantham *et al.*, 2009). FadA also forms a helical hairpin structure, but does not form dimers. Instead, the molecules form an elongated structure in what Nithianantham and coworkers describe as a leucine chain, in which the extended C-terminal helix forms a leucine-rich hydrophobic interaction with the head of the next molecule in a coiled-coil-type assembly.

5. Concluding remarks

Sundaramoorthy *et al.* (2008) make a strong case for EsxA (and, by extension, other WXG100 proteins) acting as chaperones that aid the delivery of effector proteins across the bacterial cell envelope. However, it is hard to reconcile the oligomerization we observe in the GBS1074 crystal structure with a role as chaperone. Instead, parallels with the structure of the secreted mature FadA protein hint at a possible role for GBS1074, and perhaps other WXG100 proteins, in mediating interactions with host cells. Clearly, determining whether WXG100 oligomerization occurs under physiological conditions remains a key target for research on this protein family.

References

Afonine, P. V., Grosse-Kunstleve, R. W. & Adams, P. D. (2005). *CCP4 Newsl.* **42**, contribution 8.

Arbing, M. A., Kaufmann, M., Phan, T., Chan, S., Cascio, D. & Eisenberg, D. (2010). *Protein Sci.* **19**, 1692–1703.

Burts, M. L., Williams, W. A., DeBord, K. & Missiakas, D. M. (2005). *Proc. Natl Acad. Sci. USA*, **102**, 1169–1174.

Chaudhuri, R. R., Loman, N. J., Snyder, L. A., Bailey, C. M., Stekel, D. J. & Pallen, M. J. (2008). *Nucleic Acids Res.* **36**, D543–D546.

Collaborative Computational Project, Number 4 (1994). *Acta Cryst.* D**50**, 760–763.

Emsley, P. & Cowtan, K. (2004). *Acta Cryst.* D**60**, 2126–2132.

Evans, G. & Bricogne, G. (2002). *Acta Cryst.* D**58**, 976–991.

Evans, P. R. (1993). *Proceedings of the CCP4 Study Weekend. Data Collection and Processing*, edited by L. Sawyer, N. Isaacs & S. Bailey, pp. 114–122. Warrington: Daresbury Laboratory.

Herbert, M. A., Beveridge, C. J., McCormick, D., Aten, E., Jones, N., Snyder, L. A. & Saunders, N. J. (2005). *BMC Microbiol.* **5**, 31.

Jang, S.-B., Kwon, A.-R., Son, W.-S., Park, S. J. & Lee, B.-J. (2009). *J. Biochem.* **146**, 535–540.

Kabsch, W. (2010). *Acta Cryst.* D**66**, 125–132.

Krissinel, E. & Henrick, K. (2007). *J. Mol. Biol.* **372**, 774–797.

Larsen, J. W. & Sever, J. L. (2008). *Am. J. Obstet. Gynecol.* **198**, 440–448.

Nithianantham, S., Xu, M., Yamada, M., Ikegami, A., Shoham, M. & Han, Y. W. (2009). *J. Biol. Chem.* **284**, 3865–3872.

Pallen, M. J. (2002). *Trends Microbiol.* **10**, 209–212.

Potterton, L., McNicholas, S., Krissinel, E., Gruber, J., Cowtan, K., Emsley, P., Murshudov, G. N., Cohen, S., Perrakis, A. & Noble, M. (2004). *Acta Cryst.* D**60**, 2288–2294.

Poulsen, C., Holton, S., Geerlof, A., Wilmanns, M. & Song, Y.-H. (2010). *FEBS Lett.* **584**, 669–674.

Renshaw, P. S., Lightbody, K. L., Veverka, V., Muskett, F. W., Kelly, G., Frenkiel, T. A., Gordon, S. V., Hewinson, R. G., Burke, B., Norman, J., Williamson, R. A. & Carr, M. D. (2005). *EMBO J.* **24**, 2491–2498.

Sendi, P., Johansson, L. & Norrby-Teglund, A. (2008). *Infection*, **36**, 100–111.

Sundaramoorthy, R., Fyfe, P. K. & Hunter, W. N. (2008). *J. Mol. Biol.* **383**, 603–614.

Terwilliger, T. C. (2002). *Acta Cryst.* D**58**, 1937–1940.

Vonrhein, C., Blanc, E., Roversi, P. & Bricogne, G. (2007). *Methods Mol. Biol.* **364**, 215–230.